Dynamics of Directional Selectivity in Area 18 and PMLS of the Cat

Ildikó Vajda[1,2], Martin J.M. Lankheet[1], Bart G. Borghuis[1,3] and Wim A. van de Grind[1]

[1]Department of Functional Neurobiology and Helmholtz Institute, Utrecht University, Utrecht, The Netherlands
[2]Present address: KNAW, Netherlands Institute for Brain Research, Amsterdam, The Netherlands
[3]Present address: Department of Neuroscience, University of Pennsylvania, Philadelphia, PA, USA

Visual latencies and temporal dynamics of area 18 and PMLS direction-selective complex cells were defined with a reverse correlation method. The method allowed us to analyze the time course of responses to motion steps, without confounding temporal integration effects. Several measures of response latency and direction tuning dynamics were quantified: optimal latency (OL), latency of first and last significant responses (FSR, LSR), the increase and decrease of direction sensitivity in time, and the change of direction tuning in time. FSR, OL and LSR values for PMLS and area 18 largely overlapped. The small differences in mean latencies (3–4 ms for FSR and OL and 11.9 ms for the LSR) were not statistically significant. All cells in area 18 and the vast majority of cells in PMLS showed no systematic changes in preferred direction (monophasic neurons). In PMLS 5 out of 41 cells showed a reversal of preferred direction after ~56 ms relative to their OL (biphasic neurons). Monophasic cells showed no systematic changes in direction tuning width during the interval from FSR to LSR. In both areas, development of direction sensitivity was significantly faster than return to the non-direction sensitive state, but no significant difference was found between the two areas. We conclude that, for the monophasic type of direction-selective complex cells, the dynamics of primary motion processing are highly comparable for area 18 and PMLS. This suggests that motion information is predominantly processed in parallel, presumably based on input from the fast conducting thalamocortical Y-pathway.

Keywords: cat extrastriate area, motion vision, random pixel array, reverse correlation, single unit recording

Introduction

The original view that visual information in the cat is processed hierarchically, from the retinae through area 17, area 18 and 19, up to the higher associational areas (Dreher, 1986), has been largely abandoned by now. Numerous studies have provided evidence for or suggested parallel processing rather than a hierarchical processing of visual information (e.g. Movshon *et al.*, 1978a,b,c; Thalluri and Henry, 1989; Ferster, 1990a,b; Dinse and Krüger, 1994; Katsuyama *et al.*, 1996; for overviews see Stone, 1983; Matsubara and Boyd, 2002). Important functional insights have come from comparisons of response dynamics in different areas. Dinse and Krüger (1994), for example, measured response latencies to flickering bright stimuli in several visual cortical areas of the cat and analyzed simultaneous activation patterns. They reported a high percentage of simultaneously activated cells in different areas, including areas 17, 18, 19 and some higher cortical areas.

Like in the primate visual system, several cortical areas seem to be involved in motion processing in the cat visual system. Areas 18 and the posteromedial lateral suprasylvian region (PMLS) play an important role in processing of motion (Kiefer *et al.*, 1989; Pasternak *et al.*, 1989; Spear, 1991; Pasternak and Maunsell, 1992). Whereas in primates numerous (modeling) studies discussed the origin of motion sensitive units in area MT (Sereno, 1993; Nowlan and Sejnowski, 1995; Simoncelli and Heeger, 1998; Raiguel *et al.*, 1999), not much research has been directly devoted to the same question in PMLS, which plays a similar role in the cat visual system (Payne, 1993). In addition to massive input from areas 17 and 18, PMLS also receives substantial input from a variety of thalamic nuclei (Rosenquist, 1985; Rauschecker *et al.*, 1987; for reviews see Dreher, 1986). Areas 18 and PMLS contain direction-selective complex cells (Dreher, 1986; Crook, 1990; Merabet *et al.*, 2000) and both areas are strongly (Scannell *et al.*, 1999) and reciprocally (Symonds and Rosenquist, 1984a,b) interconnected. In this paper we study to what extent differences in connectivity and interactions result in different response dynamics. Hereto, we compare complex cell response dynamics for texture motion in areas 18 and PMLS, using optimized texture motion stimuli for each cell.

To quantify the dynamics for directionally selective responses from complex cells in these areas we used a motion reverse correlation (MRC) technique (Borghuis *et al.*, 2003). The stimulus consisted of a random pixel array (RPA) performing a random walk, in which step size and delay were held constant, but directions (eight) were randomized. Spikes were reverse-correlated with the motion steps, yielding the time course of responses to each direction. The method provides a detailed description of the temporal dynamics of direction tuning and allows us to compare latencies, as well as other aspects of the dynamics of directional selectivity, such as tuning width. The motion reverse correlation technique focuses on temporal dynamics of the initial stages in motion processing, and provides a more precise and more straightforward measure of latency to moving stimuli than previously used (Orban *et al.*, 1985; Raiguel *et al.*, 1999). Because in the MRC motion direction changes after each step, confounding effects of temporal integration are minimized. The MRC method accurately reveals dynamics of motion coherence processing, and we would therefore expect clear differences in either response latencies or in response dynamics, if directional selectivity in PMLS is (partly) based on motion sensitivity in lower areas. More generally, clear differences in directional response dynamics in these areas would point to different mechanisms for direction selectivity in the two areas.

Materials and Methods

Physiological Preparation and Recording Procedure

Nine adult female cats, weighing ~3 kg each, were used in this study. The experiments were carried out according to the guidelines of the

Law on Animal Research of the Netherlands and of the Utrecht University's Animal Care and Use Committee. Anesthesia for the tracheotomy and craniotomy was induced by intramuscular injection of ketamine (15 mg/kg) and xylazine (0.5 mg/kg) (Aescoket-plus, Aesculaap BV, Leusden, The Netherlands). During recordings, anesthesia was maintained by ventilating the animal with a mixture of 70% N_2O and 30% O_2, supplemented with 0.3–0.6% halothane (Sanofi Santé BV, Maassluis, The Netherlands). Rectal temperature was monitored and maintained at 38°C with an electric heating blanket. Local analgesics in the form of Lidocaine or Xylocaine ointments (Astra Pharmaceutica BV, Zoetermeer, The Netherlands) were applied at pressure points. Heart rate, blood pressure, inspired and expired N_2O, O_2 and halothane were monitored during the experiment and, when necessary, regulated to correct ranges. Expired CO_2 was kept at 4.5–5.5%. Muscle relaxation was maintained by intravenous infusion of pancuronium bromide (Pavulon, N.V. Organon, Oss, The Netherlands) at 0.11 mg/kg per hour together with 1.94% glucose in a ringer solution.

Pupils were dilated with 1% atropine sulfate (Pharmachemie BV, Haarlem, The Netherlands) and the eyelids retracted with 2% phenylephrine hydrochloride (Veterinary Dispensary of Utrecht University, Utrecht, The Netherlands). The retinae were projected on a white screen at 57 cm distance from the eyes and the positions of the foveae were estimated from the positions of the optic disks and from the orientation of blood vessels. The eyes were focused at the appropriate viewing distance with gas-permeable, contact lenses (+3.5 to +5.0 diopter, courtesy of NKL, Emmen, The Netherlands). Focal correction was assessed by back-projection of the retinal blood vessels onto a white screen. During the experiments clarity of the optics was checked regularly.

The animal was placed in a stereotaxic apparatus (Molenaar and Van de Grind, 1980) with its head fixed by ear bars and tooth clamps. Extracellular single cell recordings from area 18 and PMLS were obtained with tungsten microelectrodes (impedance 1.0–5.4 MΩ at 500 Hz), insulated with glass or parylene (World Precision Instruments, Inc.). A craniotomy of 0.5 cm diameter was performed above area 18, at Horsley–Clarke coordinates P2-7 and ±(L1.5–L6.5). For PMLS a craniotomy of 0.8 cm was made at Horsley–Clarke coordinates A4–P4 and ±(L13–L21) (Reinoso-Suarez, 1961). For area 18, the electrode was advanced vertically, for PMLS at an angle of 30°, through an incision in the dura. Craniotomies were sealed with agar (3% in ringer solution).

Visual Stimuli

Random pixel arrays consisting of 50% bright and 50% dark pixels (Julesz, 1971) were generated by a Macintosh G4 computer. The frame rate of the stimulus monitor (Sony, Multiscan 400 PS) was 100 Hz. The mean luminance and contrast of the random pixel array were set to 50 cd/m^2 and 0.99. At the viewing distance of 57 cm and monitor resolution of 1024 × 768 pixels, the unit pixel size was 0.03 × 0.03° of visual angle. The pixel size of the RPA was always a multiple of the unit pixel size. For area 18 we mostly used a RPA pixel size of 0.24 × 0.24°, and in a few cases 0.12 × 0.12°. No differences were observed in temporal response dynamics for the different pixel sizes. Because direction-selective complex cells in area PMLS were tuned to somewhat larger pixel sizes (see also Merabet *et al.*, 2000), we mostly used a size of 0.48 × 0.48° in PMLS. Unless stated otherwise, the stimulus window measured 24 × 21°, which was large enough to cover the full receptive field.

The reverse correlation method is described in detail elsewhere (Borghuis *et al.*, 2003). In short, a RPA, covering the whole RF, moved in eight different directions, changing direction after each step. A pseudo-random sequence containing equal numbers of eight different directions was predefined by randomly shuffling the sequence of steps. The sequence usually contained a few thousands repetitions for each direction. The displacement is defined by the step size (number of unit pixels) and the delay (number of exposure frames between steps).

To obtain the time course of directional selectivity, spikes were reverse correlated with the stimulus sequence. This yielded a probability function for the occurrence of each direction of motion at each point in time preceding a spike. Figure 1*a* shows an example of the normalized probability for a single complex cell in area 18. A level of 0.125 represents chance level. Correlation between occurrence of spikes (at time 0) and motion direction is highest at about −50 ms in this example. The direction with highest relative probability corresponds to the preferred direction as measured in a classical direction tuning experiment. Figure 1*b* compares the distribution of relative probabilities at the optimal latency (peak in Fig. 1*a*) to the mean spike rate measured in 1 s stimulus intervals in which the RPA moved in the same eight directions. As shown previously (Borghuis *et al.*, 2003),

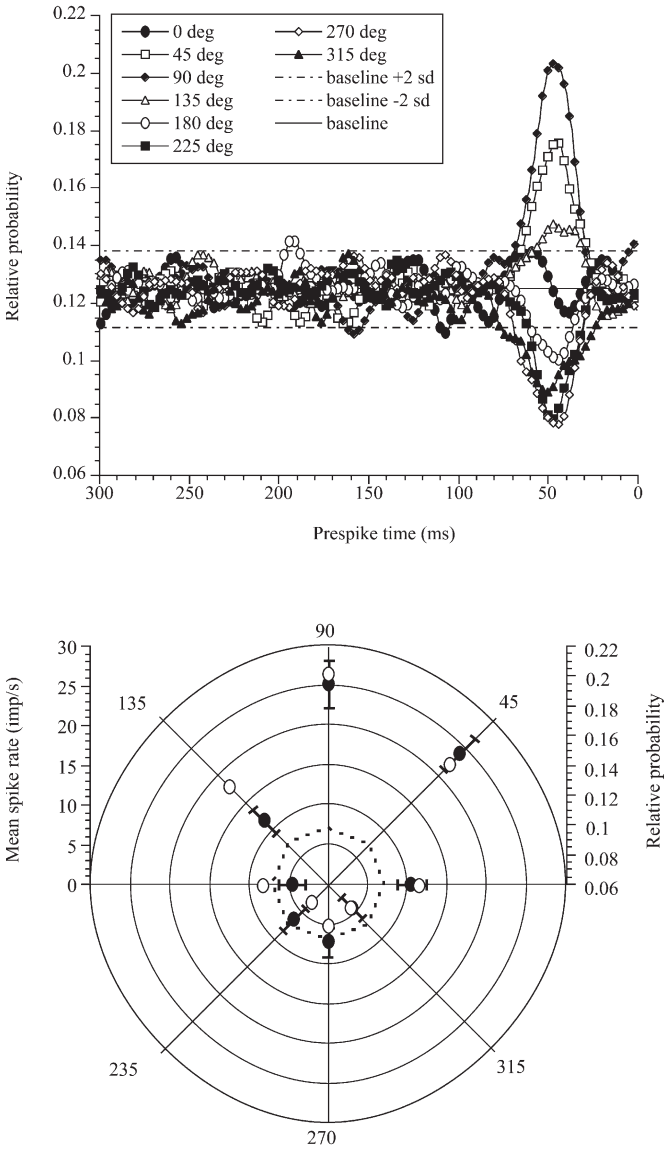

Figure 1. (*a*) Direction reverse correlogram (temporal resolution 1 ms) of an area 18 cell. Prior to the MRC experiment the V_{pref} (48°/s) and the optimal step and delay of the cell were determined. In the MRC experiment, the stimulus consisted of eight different directions and in total 15 000 motion impulses. A new direction was started after every 10 ms, during which the pattern moved coherently one element pixel (0.48°). A total of 3122 spikes were fired during the experiment. The stimulus window was 18 × 18°. The ±2 standard deviations (dashed lines) are calculated from a non-correlated part of the probability function. (*b*) Classical direction tuning experiment for the cell in *a* and the relative probabilities of the eight directions at the optimal latency from the experiment in a. In the classical direction tuning experiment (filled circles), the stimulus (element pixel size: 0.48 × 0.48°) moved in eight different directions (with 45° interval) with the V_{pref}. The dotted line indicates the level of spontaneous activity (SA), measured for a uniform gray field. Error bars represent the ±1 standard error of the means. Trial duration: 1 s, six repetitions.

preferred direction as well as tuning width correspond closely for the two methods. The reverse correlation method has the advantage that it allows us to study the dynamics of directional selectivity in great detail.

Both the time of occurrence of spikes and of motion steps were measured at a temporal resolution of 0.5 ms. This resulted in a sparse distribution of motion impulses, and therefore in somewhat noisy cross-correlation functions. Removal of this noise was achieved by smoothing the probability functions using a sliding average with a Gaussian window with a standard deviation of 5 ms (see fig. 2 in Borghuis *et al.*, 2003). The noise level in the recordings (shown as dashed lines in Fig. 1*a*) was determined from a non-correlated part of the sequence (stimuli following spikes).

Measurement Protocol

The stimulus used for searching directionally selective units consisted of a RPA of 0.12–0.48 pixel size, moving in eight different directions in 0.5 s intervals, at several different velocities. Once a single unit was isolated, two short experiments were performed to classify the cell as either 'simple' or 'complex'. The first consisted of sinusoidal gratings of different orientation and spatial frequency, moving in eight different directions. The second experiment consisted of a RPA of 0.12–0.48 pixel size, moving in eight different directions. Several different velocities were used for both experiments. Simple cells with a modulated response to drifting sinusoids were discarded. Only complex cells responding directionally selective to texture motion were used in subsequent experiments. Directional selectivity was quantified by the direction index (DI), as defined by Casanova *et al.* (1992)

$$\mathrm{DI} = 1 - \frac{\text{mean response in ND}}{\text{mean response in PD}}$$

Only complex cells with a DI of at least 0.5 were used in the present experiments (i.e. a response in the preferred direction which is at least twice as large as in the non-preferred direction). Next, the dominant eye was determined and in the case of a binocular neuron, the ipsilateral eye was covered. Subsequent experiments were performed for the dominant eye only.

In order to determine the optimal step size and delay, we first performed a standard velocity tuning experiment at the preferred direction. Velocities ranged from 0.2°/s to 384°/s. Low velocities were achieved by shifting the pattern a single unit pixel every *n*th exposure frame, high velocities by shifting the pattern *n* unit pixels each exposure frame. Next, for complex cells with sufficiently high firing frequency (>30 spikes/s) we determined the optimal step and delay combination at the optimal velocity, by using the so-called single-step pattern lifetime (SSPL) stimulus. SSPL stimuli contain motion information at a single combination of step size and delay, whereas a continuous, coherently moving pattern contains motion information at many different combinations of step size and delay. This selectivity is achieved by replacing the pattern with a new, random pattern after each coherent step. Responses were obtained for different combinations of step size and delay, all corresponding to the complex cells' preferred velocity. To minimize the jerkiness of the motion, the pattern was spatially divided in two interleaved sub-patterns that were alternately moved and refreshed. Directional selectivity at each combination of step size and delay was obtained by subtracting responses for the non-preferred direction from those to the preferred direction. Because a SSPL motion stimulus is inherently noisy and contains less motion energy than a coherently moving RPA, only highly active neurons could be driven by such a stimulus. For complex cells with low firing frequencies, for which optimal step-delay value could not be determined, we arbitrarily chose a relatively small step size and short delay value, corresponding to the preferred velocity (41 out of 73 cases).

Data Collection and Analysis

Signals were amplified (BAK Electronics, Inc.), filtered and displayed on an oscilloscope (Tektronix) and fed to an audio monitor. Spikes were detected using a window discriminator, and the resulting standardized pulses were recorded at 0.5 ms time resolution by a computer (Macintosh G4). Timing of RPA displacements was stored with the same temporal precision. Responses to direction and velocity tuning and for SSPL experiments were monitored on-line, by updating dot displays and peristimulus time histograms after each trial. During the MRC experiment, probability distributions were visualized in time and updated after every 10th spike. Spike trains and all relevant stimulus parameters were stored on disk for off-line data analysis.

MRC Data Analysis

The optimal latency and the time instances of the first and last significant responses were quantified according to Mazer *et al.* (2002). Briefly, the mean variance and its standard deviation (across directions and time) were determined from a piece of the non-correlated part of the probability function (1 s after each spike). Next, the variance for the probability functions was calculated for a 300 ms prespike interval, at 1 ms resolution. Figure 2 shows an example of the overall variance curve. It expresses the mean, squared deviation of the relative probabilities from chance level. The optimal latency (OL) was defined as the moment the variance curve reached its maximum level. The OL calculated from the variance curve corresponds closely to the time interval between stimulus and spikes at which maximal directional selectivity is obtained. The first and last significant responses (FSR, LSR) were defined as those points in time at which the variance first exceeded, respectively fell below the level of two standard deviations (of the mean variance of the non-correlated part).

In addition to the latencies based on the overall variance curves we used several different measures to characterize and compare the temporal dynamics of directional selectivity in the two areas. To specifically quantify the increase and decline of directional sensitivity, lines were fitted to the rising (points between FSR and OL) and falling (points between OL and LSR) phase of the overall variance curves. The slope-values of these lines represent the speed at which directional sensitivity changes. Since in the variance curve directions are pooled together, the change of directional sensitivity does not necessarily reflect a change in directional selectivity. Moreover, the overall variance curves provide no information on the variability of preferred directions. To quantify the preferred direction during the 300 ms response window we used the vector sum of probabilities for all directions. The resulting directional vector sum (DV) represents the preferred direction and the strength of directional selectivity, taking all eight possible directions into account. The width of direction tuning was determined by fitting Gaussian direction tuning profiles to the probabilities as a function of direction, at each point in time. Because low relative probabilities yielded noise estimates of tuning width, we limited the analysis to a time window of 10 ms before and

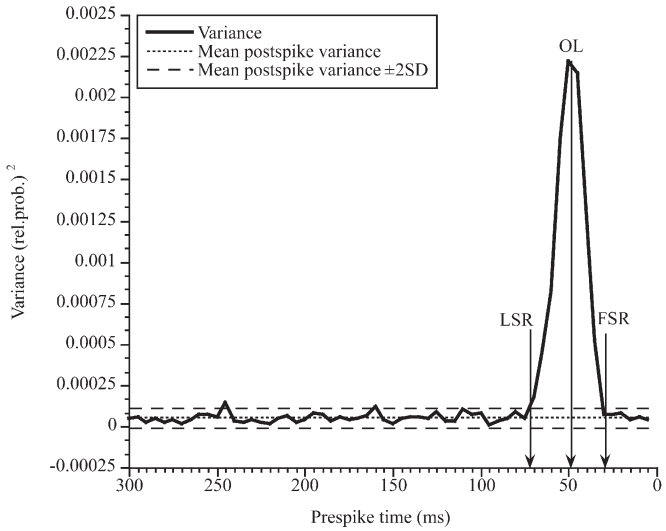

Figure 2. Overall variance plot of the probability functions for the cell in Figure 1*a*. Mean postspike variance and its standard deviation are calculated from a non-correlated portion of the probability functions. Optimal latency (OL), first significant response (FSR) and last significant response (LSR) are marked by arrows.

after the optimal latency. For a number of complex cells (9 in area 18 and 3 in PMLS), fits at some time points (mostly at 9 ms and 10 ms before or after the OL) yielded a low correlation coefficient ($R < 0.8$). We discarded these cells from further analysis. For the remaining cells, the width of direction tuning is quantified by the σ of the fitted Gaussian.

Results

Population Response Characteristics

In area 18, MRC experiments were performed on 32 neurons, in PMLS on 41 neurons. The average DI for area 18 complex cells was 0.80, for PMLS it was 0.76. In area 18, preferred velocities varied from 6°/s to 72°/s, in PMLS from 3°/s to 192°/s. The reverse correlogram shown in Figure 1*a* is exemplary for all area 18 complex cells and for the vast majority of PMLS complex cells. Typically, the variance curve showed a single peak. In PMLS, however, five complex cells were encountered, that showed a second peak in the variance curve. Figure 3*a* shows an example of direction tuning for such a 'biphasic' cell. The figure represents the directional vector sum (DV) plotted on a time axis, showing the change in time of directional selectivity (length of the vector) and of preferred direction. Figure 3*b* shows a DV plot for the area 18 cell from Figures 1 and 2. Biphasic type of cells has also been found in macaque area MT (Borghuis *et al.*, 2003) where they constitute ~50% of the total population. Because in PMLS biphasic cells form a small, distinctive subgroup, we did not include these cells in the comparison of population characteristics between area 18 and PMLS. In a future study we will specifically address the distinctive response properties of these so-called biphasic cells.

Figure 4 shows the variance curve, averaged for all area 18 complex cells and for all monophasic complex cells in area PMLS. Directional selectivity is slightly higher in area 18 than in PMLS, just as it was found by using the classical directional tuning method (see previous paragraph). Mean variance in area 18 reached ~0.003 at its optimum. In PMLS the mean optimal

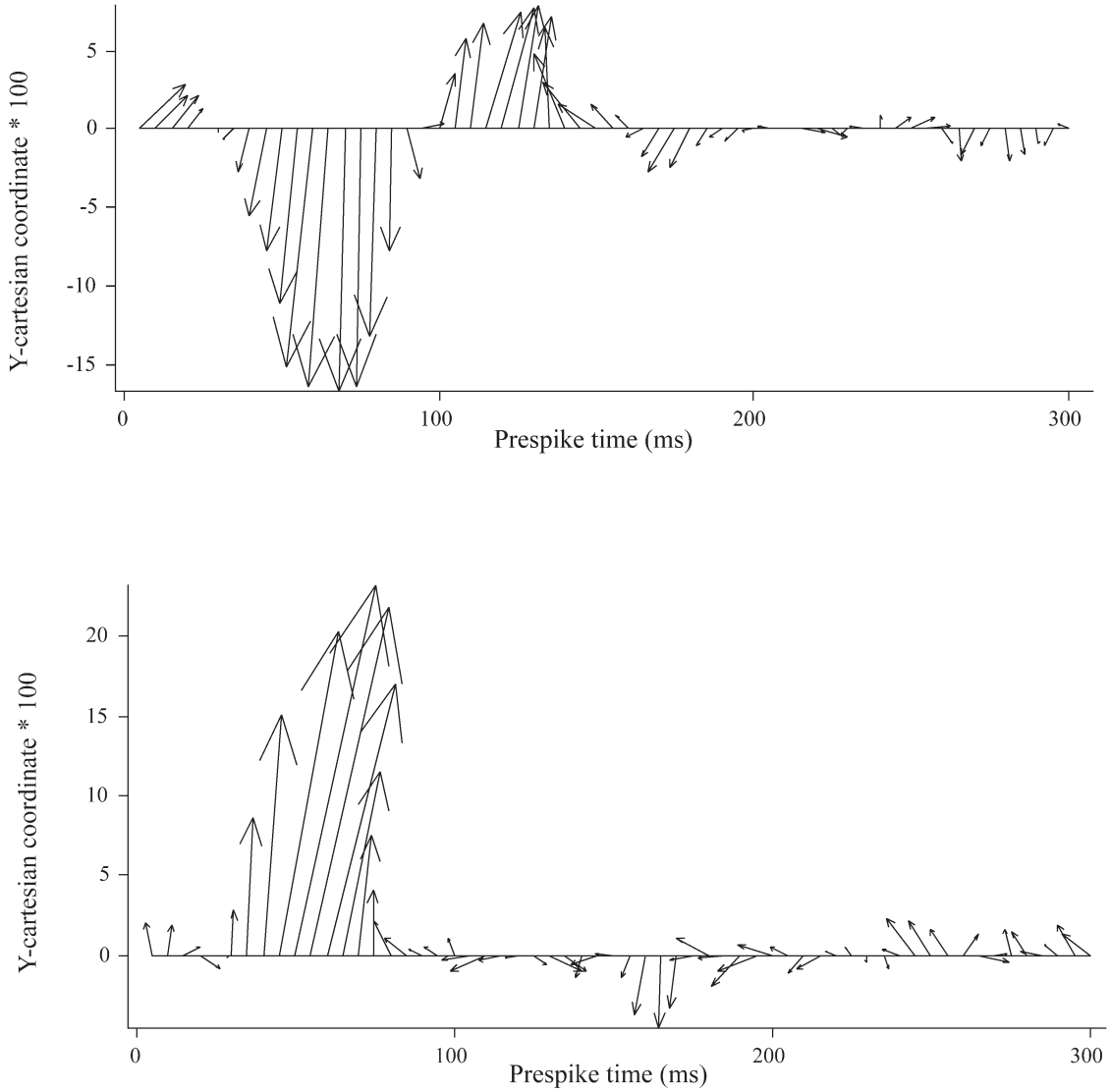

Figure 3. Directional vector sum plots as a function of prespike time of a biphasic PMLS complex cell (*a*) and of the monophasic area 18 cell (*b*) from Figures 1, 2 and 3. At each time instance of the probability function (temporal resolution 1 ms), the direction vectors of the eight different directions were summed. The magnitude and direction of the resulting sum of the vectors is plotted for every 5 ms. Therefore the origins of the DVs are equally spaced. The magnitude of a DV is given in Cartesian coordinates and indicated only for the *y*-coordinate (multiplied by 100 for visibility). An *x*-coordinate can be found by drawing a perpendicular line from the end of a DV to the time axis.

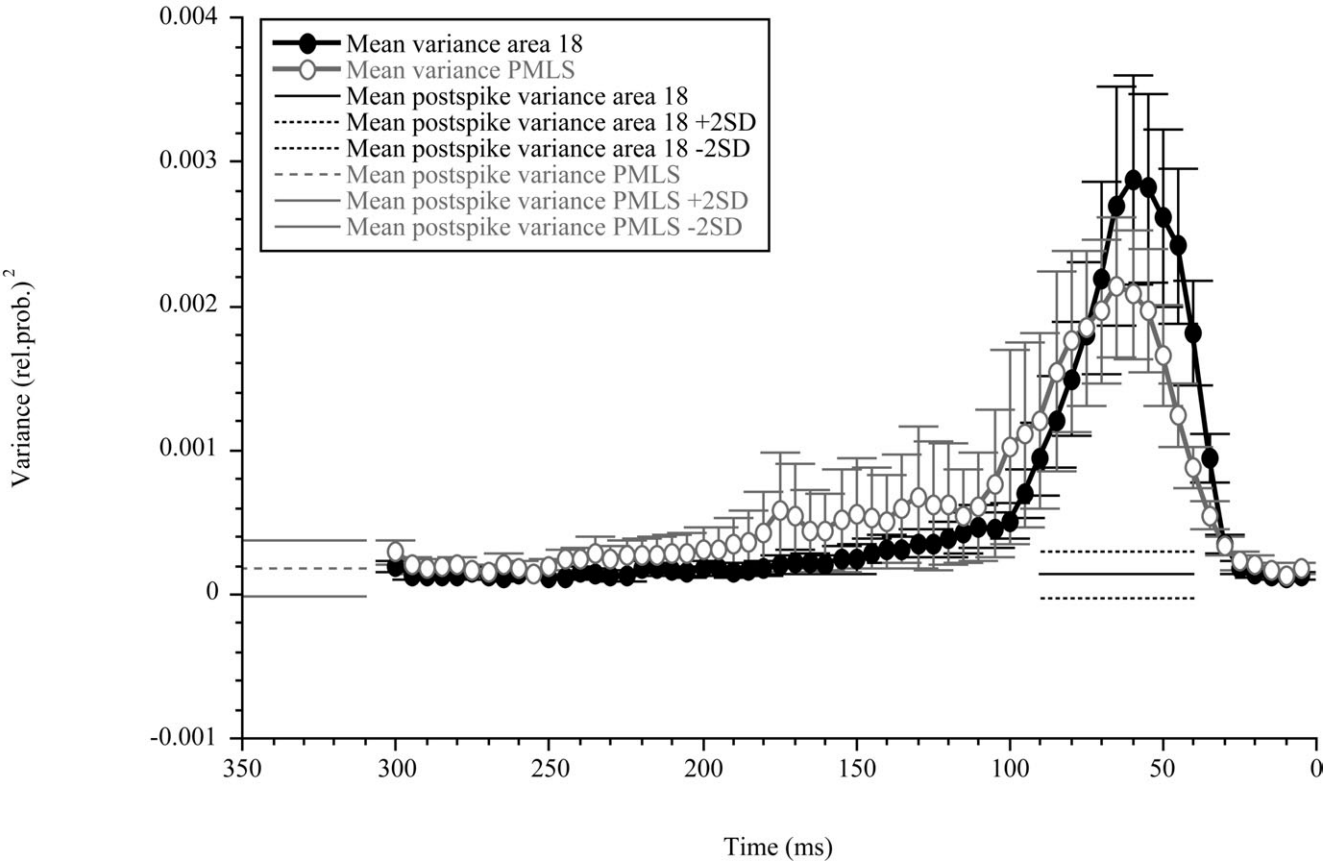

Figure 4. Mean overall variance curves of 32 area 18 complex cells (solid dots) and 36 PMLS complex cells (open dots). Mean postspike variances are the means of the mean postspike variances of individual cells, which were calculated from the non-correlated portion of the probability functions (see Materials and Methods). Error bars represent ±1 SEM.

variance was ~27% lower (0.0022). Apart from this clear difference, there were no obvious substantial differences in response profiles between the two areas. In Figures 5 and 6 we quantitatively compare response latencies based on the same data underlying the variance curves in Figure 4.

Figure 5*a* shows the latency of the first significant response (FSR), i.e. the minimal time required for the response to surpass the level of the mean post-spike variance plus two standard deviations. Mean variance and its standard deviations are based on 1 s post-spike correlations, reflecting noise in the uncorrelated part of the sequences (see Figs 2 and 4). The mean FSR in PMLS (34.2 ms) was slightly longer than in area 18 (30.8 ms). Figure 4 shows that this difference partly results from a slightly higher noise level in PMLS, and from a slower increase of the variance. A similar difference between the two areas was found for the optimal latencies. Mean optimal latency was 59.1 ms in PMLS and 55.8 ms in area 18. For the LSR the opposite was observed: area 18 had a longer mean LSR (108.6 ms) than PMLS (96.7 ms). Figure 5*c* shows that there was substantial scatter in the LSR latency values. Large scatters are common in latency studies (Ikeda and Wright, 1975; Best *et al.*, 1986; Raiguel *et al.*, 1989, 1999; Maunsell and Gibson, 1992; Dinse and Krüger, 1994; Saul and Feidler, 2002), and their range depends partly on the diversity and extensiveness of inputs to an area. None of the observed latency differences between areas, however, turned out to be significant (P(OL) > 0.2; P(FSR) > 0.1; P(LSR) > 0.1).

In our study, part of the scatter might also have been caused by differences in stimulus-delay, which was optimized for about half of the neurons (see Materials and Methods). In area 18, delay values varied between 10 ms and 80 ms, in PMLS between 10 and 160 ms. For short delays motion steps follow each other rapidly, creating an opportunity for temporal interactions. Cells mostly fired single spikes in response to individual steps in a fast sequence. For long delays the opportunity for temporal interactions were less, which resulted in slightly longer responses to steps in the preferred direction. The resulting increase in latency values with stimulus delay was however very modest and turned out to be non-significant within an area. Only area 18 OL values measured with 10 and 40 ms and with 10 and 20 ms and PMLS LSR values measured with 10 and 20 ms yielded a small but significant difference.

Direction Tuning Dynamics

Analysis of the directional vector sum (DV) as a function of prespike interval showed no systematic variation in preferred direction. Apart from five biphasic cells (Fig. 3*a*) that reverse their preferred direction for longer prespike intervals, cells in area 18 and monophasic PMLS neurons showed no systematic change of preferred directions. In both areas, the majority of the cells showed little or no variation in the angle. Few cells showed small, but non-systematic changes. No differences were observed between the change of directions for monophasic cells in area 18 and in PMLS.

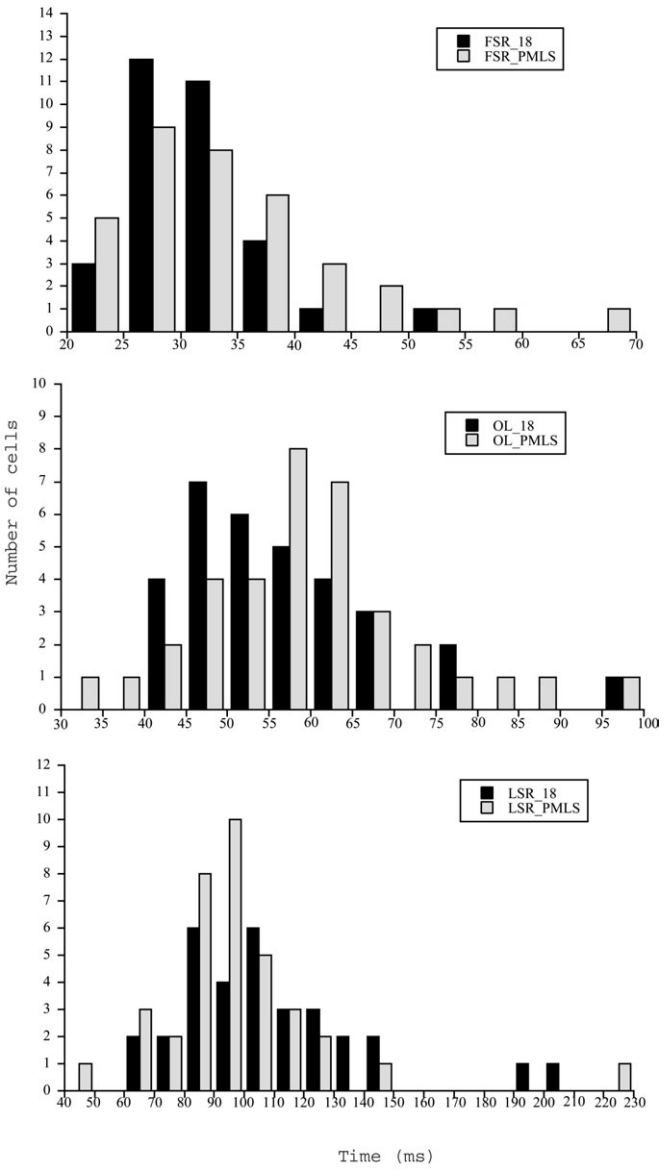

Figure 5. FSR, OL and LSR distributions of 32 area 18 and 36 PMLS complex cells, following stimulation with MRC, making one step in each direction. Stimulus parameters varied per cell, depending on its preferred velocity and optimal step–delay combination (see Materials and Methods for further details).

To compare the velocity of increase and decrease of directional sensitivity we determined the slopes of the lines fitted to the points between the FSR and OL and OL and LSR of the variance curves. Mean correlation coefficient (R) for fits to the rising part was 0.95 (SD = 0.07) in area 18 and 0.93 (SD = 0.11) in PMLS. Mean correlation coefficients for the interval from OL to LSR were 0.89 (SD = 0.08) for area 18 and 0.92 (SD = 0.07) for PMLS. Figure 6 compares the distribution of slopes for the two areas. Slopes were normalized to the maximum variance level at the optimal latency.

Within each area, the mean slope of the increasing part was significantly steeper than the mean slope for the decreasing part ($P < 0.0001$ for area 18; $P < 0.002$ for PMLS). No significant differences were found in the increasing and decreasing mean slope values between the areas ($P > 0.2$ for increasing and $P > 0.4$ for decreasing part). These results show that both in area 18 and in PMLS directional sensitivity increases faster than it decreases.

Finally, we analyzed to what extent the sharpness of the direction tuning changes during the course of the response profile. Does the tuning width change in time, and if so, is this different for areas 18 and PMLS? We determined the change in width as a function of time, for a 10 ms interval before and after the optimal latency. To this end, we determined the σ of the fitted Gaussian to the relative probability points (see Materials and Methods). In Figure 7 the mean σ and its standard deviation is shown for a population of 23 area 18 and 31 PMLS complex cells.

No substantial changes in the mean σ values were found in the 10 ms period before and after the OL within or between the areas. For individual neurons, no systematic change in σ values was seen in the 10 ms period around the OL: some cells showed a slight sharpening of their tuning at the OL, some continued to sharpen their tuning beyond the time of the OL, however the majority of the cells did not change their tuning width in the whole period.

Discussion

We found no significant differences in the mean latency values (FSR, OL, LSR) between area 18 and PMLS complex cells for moving texture patterns. For non-moving, flickering stimuli, Dinse and Krüger (1994) did find a significant ($P < 0.00001$) difference in mean response latencies between area 18 (mean: 40.4 ms; SD = 9.4 ms) and PMLS (mean: 66.7 ms; SD = 23.2 ms). They found lengthening in the mean latency in the following order: LGN (37.9 ms; SD = 7.1 ms), area 18, area 17 (52.7 ms; SD = 19.6 ms), PMLS, area 7 (83.5 ms; SD = 31.8 ms), area 19 (93.6 ms; SD = 29.6 ms). Despite the significant differences in response latencies, most neurons at different stages were simultaneously active, due to variations in latency within each area and the duration of responses to bright flickering stimuli. For our moving stimuli, the difference in the mean OL between area 18 and PMLS was only 3.3 ms, which is considerably less than the 26.3 ms found for flickering stimuli by Dinse and Krüger (1994).

What do these different results mean in terms of stimulus specific responses? It has been shown that subcortical latency measurements depend on stimulus parameters such as spatial frequency and contrast (Bolz *et al.*, 1982; Sestokas and Lehmkuhle, 1986), location of the stimulus within the RF (Bolz *et al.*, 1982; Orban *et al.*, 1985), the size of the stimulus and the background illumination (Bolz *et al.*, 1982). Using the same visual stimulus in different cortical areas, as in the study of Dinse and Krüger, may therefore result in latency differences due to quantitative differences in tuning properties. Suboptimal stimuli may even reverse the order of response latencies in different types of neurons, like in the case of retinal X- and Y-cells (Bolz *et al.*, 1982). In contrast to the study of Dinse and Krüger (1994), we optimized the stimuli for each complex cell and stimulated the entire RF, which excludes large differences due to difference in stimulus efficacy.

The small, nonsignificant differences in response latencies between area 18 and PMLS support parallel motion coherence detection in the two areas. Dinse and Krüger (1994) also argued that their data did not imply a major role for serial processing. Assuming a signal propagation time of 5–15 ms between different processing stages, the differences they

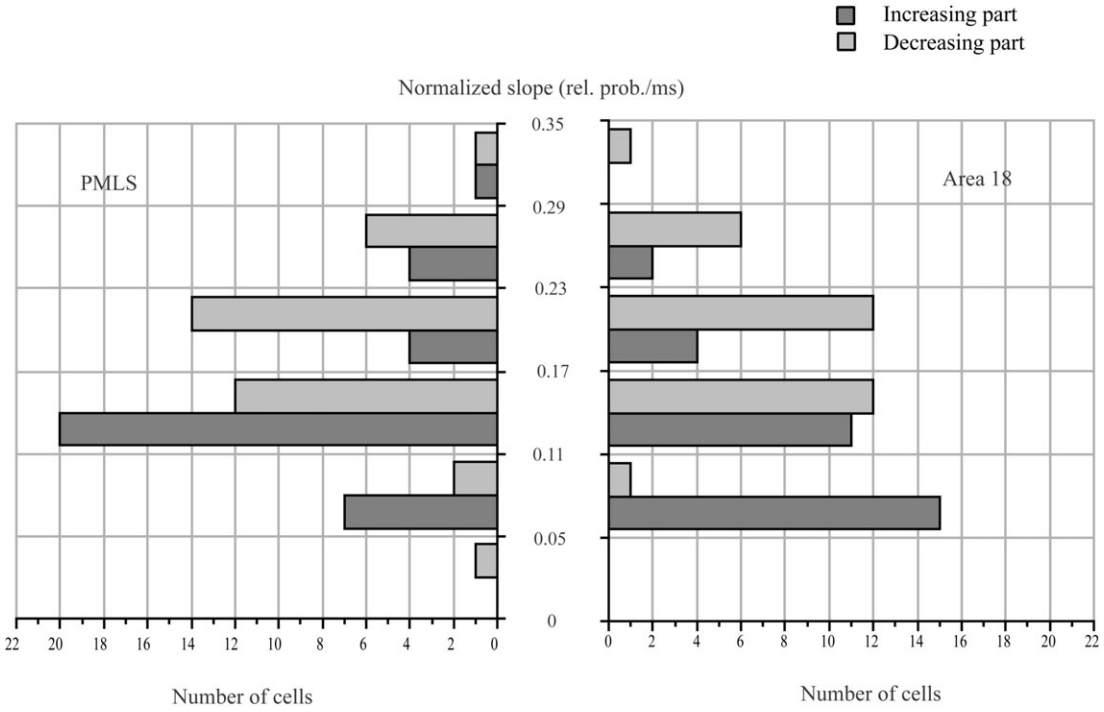

Figure 6. Frequency distributions of the slopes of lines, fitted to the overall variance curves in both areas. Slope values were normalized by dividing them by the variance at the time of OL.

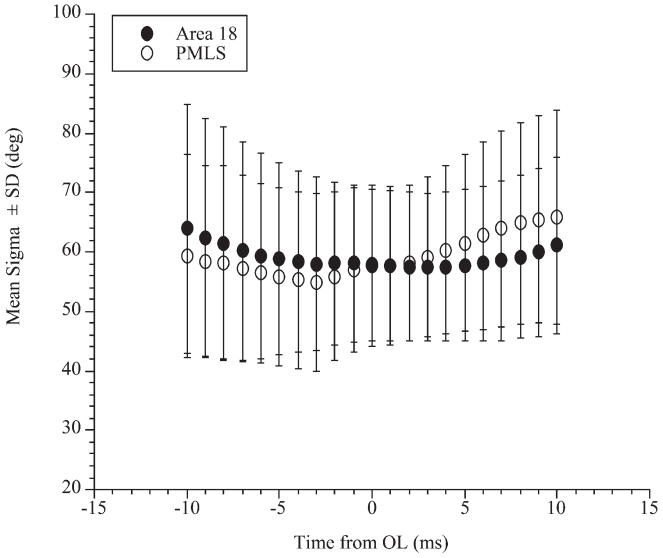

Figure 7. Mean sigma values plotted as a function of time 10 ms before and 10 ms after the optimal latency. Filled circles represent area 18, open circles represent PMLS data. Error bars represent ±1 SEM.

found (which were between 2.5 ms and 16.8 ms; see order of activation in the first paragraph of this section) were small relative to the variation within each area. The latency difference of 26.3 ms between area 18 and PMLS would however suggest significantly different mechanisms and a contribution from serial processing, that would be in line with the fact that they are extensively interconnected (Scannell *et al.*, 1999). Our data, specifically concerning motion detection, however do not favor serial processing of motion processing in the two areas. For optimized stimuli, probing primary motion coherence detection, we found no significant latency differences between complex cells in area 18 and PMLS. Although our data do not exclude a contribution from serial processing, they argue for a dominant role of parallel, simultaneous motion detection in the two areas.

Numerous studies have described the thalamocortical projections to area 18 and PMLS. We will not discuss the anatomy in detail, but two important findings need to be mentioned. First, it has been shown, that PMLS neurons are predominantly driven by the Y-cell pathway (Wang *et al.*, 1997), either directly through the LP–pulvinar complex (Rauschecker *et al.*, 1987) or by direct Y-cell input from the LGN (Berson, 1985). Similarly, area 18 neurons are driven by the Y-cell pathway mainly through the LGN (Sherman, 1985) some of them monosynaptically (Harvey, 1980). Similarly to PMLS, area 18 also receives direct Y-pathway input from extrageniculate subcortical areas like the LP–pulvinar complex (Rackowski and Rosenquist, 1983). We suggest, that the similarity of FSRs and OLs in area 18 and PMLS, and their relatively small scatter in our study, probably reflect input from the fast conducting Y-pathway to both areas. Whether our population of complex cells in these areas reflects direct or indirect afferent input through the Y-pathway remains to be explored.

The simultaneous activation of the majority of directionally selective complex cells in area 18 and PMLS suggests that motion sensitivity in PMLS does not (entirely) depend on area 18. This is in line with the finding reported by Rauschecker *et al.* (1987) that direction-selective PMLS neurons receive direct input from fast conducting Y-type cells from the lateral posterior nucleus (LP). The same study, however also provided evidence for a role of striate cortex in generating PMLS directional selectivity. Minville and Casanova (1998) furthermore

showed that deactivation of LP did not alter direction selectivity in PMLS, suggesting that LP is not necessary for direction selectivity in PMLS. On the other hand, lesioning area 17 and area 18 did not reduce direction-selective cells in PMLS (Guedes *et al.*, 1983; but see Spear and Baumann, 1979; Guido *et al.*, 1990). Our latency results support the hypothesis that direction selectivity in PMLS does not exclusively result from cortical direction selectivity at lower cortical levels. It seems that most PMLS complex cells derive their directional selectivity from non-directionally selective input form the thalamus. Possibly, lagged and non-lagged cells in the thalamus play a role in providing timing differences. For area 17 simple cells, input from lagged and non-lagged X-cells has been indicated (Saul and Humphrey, 1990; Jagadeesh *et al.*, 1997; Saul and Feidler, 2002). Lagged and non-lagged Y-cells (Saul and Humphrey, 1990; Mastronarde *et al.*, 1991) might play a similar role in both area 18 and PMLS.

The similarity in temporal dynamics of directional selectivity between area 18 and PMLS provides further support for similar motion detection mechanisms. The asymmetry between rising and falling phases was similar in both areas: increases in directional sensitivity were faster than decreases. The similarity points at similar roles for temporal integration in both areas in establishing directional selectivity. Temporal dynamics of direction sensitivity showed more variation within each area, than between the areas, suggesting that similar local circuitry is involved in developing and phasing out direction sensitivity of complex cells. This is further supported by the absence of changes in direction tuning widths in both areas. In both areas there was an extended time period (at least 20 ms) in which the width of the tuning remains fairly constant.

In this study we showed that area 18 and PMLS did not differ significantly in their temporal dynamics for coherence detection of texture motion. In this respect, these areas seem to be more similar than expected based on previously reported anatomical and electrophysiological data. A minority of PMLS complex cells however did show deviating temporal dynamics. Biphasic cells that were only encountered in PMLS reversed their preferred direction, which makes them especially sensitive to motion contrast (motion reversals). Thus, PMLS not only shows more sophisticated spatial RFs than areas 17 and 18 (Von Grünau and Frost, 1983; Toyama *et al.*, 1985, 1991; Von Grünau *et al.*, 1987; Niida *et al.*, 1997), but also in the temporal domain.

Notes

Address correspondence to Ildikó Vajda, NIBR (KNAW), Neurons and Networks Group, Meigbergdreef 33, 1105 AZ Amsterdam, The Netherlands. Email: i.vajda@nih.knaw.nl.

References

Berson DM (1985) Cat lateral suprasylvian cortex: Y-cell inputs and corticotectal projection. J Neurophysiol 53:544–556.

Best J, Reuss S, Dinse HR (1986) Lamina-specific differences of visual latencies following photic stimulation in the cat striate cortex. Brain Res 385:356–360.

Bolz J, Rosner G, Wassle H (1982) Response latency of brisk-sustained (X) and brisk-transient (Y) cells in the cat retina. J Physiol (Lond) 328:171–190.

Borghuis BG, Perge JA, Vajda I, Van Wezel RJA, Van de Grind WA, Lankheet MJM (2003) The motion reverse correlation method: a linear systems approach in the motion domain. J Neurosci Methods 123:153–166.

Casanova C, Nordmann JP, Ohzawa I, Freeman RD (1992) Direction selectivity of cells in the cat's striate cortex: differences between bar and grating stimuli. Vis Neurosci 9:505–513.

Crook JM (1990) Directional tuning of cells in area 18 of the feline visual cortex for visual noise, bar and spot stimuli: a comparison with area 17. Exp. Brain Res 80:545–561.

Dinse HR, Krüger K (1994) The timing of processing along the visual pathway in the cat. Neuroreport 5:893–897.

Dreher B (1986) Thalamocortical and corticocortical interconnections in the cat visual system: relation to the mechanisms of information processing. In: Visual neuroscience (Pettigrew JD, Sanderson KJ, Levick WR, eds), pp. 290–314. Cambridge: Cambridge University Press.

Ferster D (1990a) X-and Y-mediated synaptic potentials in neurons of area 17 and 18 of cat visual cortex. Vis Neurosci 4:115–133.

Ferster D (1990b) X-and Y-mediated current sources in neurons of area 17 and 18 of cat visual cortex. Vis Neurosci 4:135–145.

Guedes R, Watanabe S, Creutzfeldt OD (1983) Functional role of association fibres for a visual association area: the posterior suprasylvian sulcus of the cat. Exp Brain Res 49:13–27.

Guido W, Tong L, Spear PD (1990) Afferent bases of spatial- and temporal-frequency processing by neurons in the cat's posteromedial lateral suprasylvian cortex: effects of removing areas 17, 18, and 19. J Neurophysiol 64:1636–1651.

Harvey AR (1980) The afferent connexions and laminar distribution of cells in area 18 of the cat. J Physiol (Lond) 302:483–505.

Ikeda I, Wright MJ (1975) Retinotopic distribution, visual latency and orientation tuning of 'sustained' and 'transient' cortical neurons in area 17 of the cat. Exp Brain Res 22:385–398.

Jagadeesh B, Wheat HS, Kontsevich LL, Tyler CW, Ferster D (1997) Direction selectivity of synaptic potentials in simple cells of the cat visual cortex. J Neurophysiol 78:2772–2789.

Julesz B (1971) Foundations of cyclopean perception. Chicago, IL: University of Chicago Press.

Katsuyama N, Tsumoto T, Sato H, Fukuda M, Hata Y (1996) Lateral suprasylvian visual cortex is activated earlier than or synchronously with primary visual cortex in the cat. Neurosci Res 24:431–435.

Kiefer W, Kruger K, Strauss G, Berlucchi G (1989) Considerable deficits in the detection performance of the cat after lesion of the suprasylvian visual cortex. Exp Brain Res 75:208–212.

Mastronarde DN, Humphrey AL, Saul AB (1991) Lagged Y cells in the cat lateral geniculate nucleus. Vis Neurosci 7:191–200.

Matsubara JA, Boyd JD (2002) Relationship of LGN afferents and cortical efferents to cytochrome oxidase blobs. In: The cat primary visual cortex (Payne BR, Peters A, eds), pp. 221–258. London: Academic Press.

Maunsell JH, Gibson JR (1992) Visual response latencies in striate cortex of the macaque monkey. J Neurophysiol 68:1332–1344.

Mazer JA, Vinje WE, McDermott J, Schiller PH, Gallant JL (2002) Spatial frequency and orientation tuning dynamics in area V1. Proc Natl Acad Sci USA 99:1645–1650.

Merabet L, Minville K, Ptito M, Casanova C (2000) Responses of neurons in the cat posteromedial lateral suprasylvian cortex to moving texture patterns. Neuroscience 97:611–623.

Minville K, Casanova C (1998) Spatial frequency processing in posteromedial lateral suprasylvian cortex does not depend on the projections from the striate-recipient zone of the cat's lateral posterior–pulvinar complex. Neuroscience 84:699–711.

Molenaar J, Van de Grind WA (1980) A stereotaxic method of recording from single neurons in the intact *in vivo* eye of the cat. J Neurosci Methods 2:135–152.

Movshon JA, Thompson ID, Tolhurst, DJ (1978a) Spatial summation in the receptive fields of simple cells in the cat's striate cortex. J Physiol (Lond) 283:53–77.

Movshon JA, Thompson ID, Tolhurst, DJ (1978b) Receptive field organization of complex cells in the cat's striate cortex. J Physiol (Lond) 283:79–99.

Movshon JA, Thompson ID, Tolhurst, DJ (1978c) Spatial and temporal contrast sensitivity of neurones in areas 17 and 18 of the cat's visual cortex. J Physiol (Lond) 283:101–120.

Niida T, Stein BE, McHaffie JG (1997) Response properties of corticotectal and corticostriatal neurons in the posterior lateral suprasylvian cortex of the cat. J Neurosci 17:8550–8565.
Nowlan SJ, Sejnowski TJ (1995) A selection model for motion processing in area MT of primates. J Neurosci 15:1195–1214.
Orban GA, Hoffmann KP, Duysens J (1985) Velocity selectivity in the cat visual system. I., Responses of LGN cells to moving bar stimuli: a comparison with cortical areas 17 and 18. J Neurophysiol 54:1026–1049.
Pasternak T, Maunsell JH (1992) Spatiotemporal sensitivity following lesions of area 18 in the cat. J Neurosci 12:4521–4529.
Pasternak T, Horn KM, Maunsell JH (1989) Deficits in speed discrimination following lesions of the lateral suprasylvian cortex in the cat. Vis Neurosci 3:365–375.
Payne BR (1993) Evidence for visual cortical area homologs in cat and macaque monkey. Cereb Cortex 3:1–25.
Rackowski D, Rosenquist AC (1983) Connections of the multiple visual cortical areas with the lateral posterior–pulvinar complex and adjacent thalamic nuclei in the cat. J Neurosci 3:1912–1942.
Raiguel SE, Lagae L, Gulyas B, Orban GA (1989) Response latencies of visual cells in macaque areas V1, V2 and V5. Brain Res 493:155–159.
Raiguel SE, Xiao DK, Marcar VL, Orban GA (1999) Response latency of macaque area MT/V5 neurons and its relationship to stimulus parameters. J Neurophysiol 82:1944–1956.
Rauschecker JP, von Grunau MW, Poulin C (1987) Thalamo-cortical connections and their correlation with receptive field properties in the cat's lateral suprasylvian visual cortex. Exp Brain Res 67:100–112.
Reinoso-Suarez F (1961) Topografischer Hirnatlas der Katze fuer experimental-physiologische untersuchung. Darmstadt: E. Merck AG.
Rosenquist AC (1985) Connections of visual cortical areas in the cat. In: Cerebral cortex (Peters A, Jones EG, eds), pp. 81–117. NewYork: Plenum.
Saul AB, Feidler JC (2002) Development of response timing and direction selectivity in cat visual thalamus and cortex. J Neurosci 22:2945–2955.
Saul AB, Humphrey AL (1990) Spatial and temporal response properties of lagged and nonlagged cells in cat lateral geniculate nucleus. J Neurophysiol 64:206–224.
Scannell JW, Burns GA, Hilgetag CC, O'Neil MA, Young MP (1999) The connectional organization of the cortico-thalamic system of the cat. Cereb Cortex 9:277–299.
Sereno ME (1993) Neuronal computation of pattern motion: modeling stages of motion analysis in the primate visual cortex. Cambridge, MA: MIT Press.
Sestokas AK, Lehmkuhle S (1986) Visual response latency of X- and Y-cells in the dorsal lateral geniculate nucleus of the cat. Vision Res 26:1041–1054.
Sherman SM (1985) functional organization of the W-, X- and Y-cell pathways in the cat, a review and hypothesis. In: Progress in psychobiology and physiological psychology (Sprague JM, Epstein AN, eds), pp. 233–314. New York: Academic Press.
Simoncelli EP, Heeger DJ (1998) A model of neuronal responses in visual area MT. Vision Res 38:743–761.
Spear PD (1991) Functions of extrastruate visual cortex in non-primate species. In: The neural basis of visual dysfunction (Leventhal AG, ed.), pp. 339–370. New York: Macmillan Press.
Spear PD, Baumann TP (1979) Effects of visual cortex removal on receptive-field properties of neurons in lateral suprasylvian visual area of the cat. J Neurophysiol 42:31–56.
Stone J (1983) Parallel processing in the visual system. New York: Plenum.
Symonds LL, Rosenquist AC (1984a) Corticocortical connections among visual areas in the cat. J Comp Neurol 229:1–38.
Symonds LL, Rosenquist AC (1984b) Laminar origins of visual corticocortical connections in the cat. J Comp Neurol 229:39–47.
Thalluri J, Henry GH (1989) Neurons of the cat striate cortex driven transsynaptically by electrical stimulation of the superior colliculus. Vision Res 29:1319–1323.
Toyama K, Komatsu Y, Kasai H, Fujii K, Umetani K (1985) Responsiveness of Clare–Bishop neurons to visual cues associated with motion of a visual stimulus in three-dimensional space. Vision Res 25:407–414.
Toyama K, Kitaoji H, Umetani K (1991) Binocular neuronal responsiveness in Clare–Bishop cortex of Siamese cats. Exp Brain Res 86:471–482.
Von Grünau M, Frost BJ (1983) Double-opponent-process mechanism underlying RF-structure of directionally specific cells of cat lateral suprasylvian visual area. Exp Brain Res 49:84–92.
Von Grünau M, Zumbroich TJ, Poulin C (1987) Visual receptive field properties in the posterior suprasylvian cortex of the cat: a comparison between areas PMLS and PLLS. Vision Res 27:343–356.
Wang C, Dreher B, Huxlin KR, Burke W (1997) Excitatory convergence of Y and non-Y information channels on single neurons in the PMLS area, a motion area of the cat visual cortex. Eur J Neurosci 9:921–933.
Zumbroich TJ, von Grunau M, Poulin C, Blakemore C (1986) Differences of visual field representation in the medial and lateral banks of the suprasylvian cortex (PMLS/PLLS) of the cat. Exp Brain Res 64:77–93.